CHEMPHYSCHEM

Supporting Information

Monomer Dynamics of Alzheimer Peptides and Kinetic Control of Early Aggregation in Alzheimer's Disease

Srabasti Acharya,[a] Kinshuk R. Srivastava,[a] Sureshbabu Nagarajan,[a] and Lisa J. Lapidus*[a, b]

cphc_201600706_sm_miscellaneous_information.pdf

Model of Oligomer Formation

The premise for the model below is that each peptide monomer can adopt a variety of conformations through intramolecular diffusion. These conformations can be divided into two states, those that have hydrophobic patches exposed to solvent (M^*) and those that don't (M). Only those that have hydrophobic patches exposed to solvent can make stable dimers. A full model of all dimers that can be formed is

$$
\begin{array}{ccccc}
M & \underset{k_{-1}}{\overset{k_1}{\rightleftarrows}} & M^* & & \\
M^* + M^* & \underset{k_d}{\overset{k_+^{bi}}{\rightleftarrows}} & [M^*M^*] & \underset{k_{-O}}{\overset{k_O}{\rightleftarrows}} & O \\
 & & k_1 \updownarrow k_{-1} & & \\
M + M^* & \underset{k_-^{bi}}{\overset{k_+^{bi}}{\rightleftarrows}} & [MM^*] & & \\
 & & k_1 \updownarrow k_{-1} & & \\
M + M & \underset{k_-^{bi}}{\overset{k_+^{bi}}{\rightleftarrows}} & [MM] & &
\end{array}
\qquad \text{(i)}
$$

We make several assumptions:

1) The formation of O is irreversible; that is, $k_{-O} \sim 0$
2) $k_O << k_+^{bi}$.
3) It is not possible to measure the reconfiguration of encounter complexes, since they are extremely unstable. We assume that their reconfiguration is the same as for the monomers, as they comprise of loosely bound monomers.
4) Since there are no stabilizing interactions for $[MM]$ and $[MM^*]$, the dissociation rate, k_-^{bi}, for these complexes is purely diffusive.
5) Bimolecular dissociation constants depend on the stabilizing interactions of the encounter complex. k_d is much smaller than k_-^{bi} because there are attractive hydrophobic interactions in $[M^*M^*]$.

To avoid going irreversibly to *O*, [*M*M**] can dissociate to *M** and *M** or reconfigure to [*MM**]. Thus, for $k_{-1} >> k_d$, the primary flux of dissociation is through [MM*]. This complex is not very stable and so immediately comes apart. Therefore we assume that [*M*M**] can proceed directly to *M*+*M**. Thus, for k_{-O} and k_d sufficiently slow, and k_-^{bi} sufficiently fast, the model can be approximated by scheme (ii), which has been used in previous versions of this model [1]

$$\begin{array}{l} M \underset{k_{-1}}{\overset{k_1}{\rightleftarrows}} M^* \\ M^* + M^* \xrightarrow{k_{bi}} [M^* M^*] \xrightarrow{k_O} O \\ \qquad\qquad\quad \downarrow k_{-1} \\ \qquad\qquad\quad M + M^* \end{array} \qquad \text{(ii)}$$

The equations of the full model (scheme (i)) are

$$\begin{aligned}
\frac{d[M]}{dt} &= -k_1[M] + k_{-1}[M^*] - 2k_+^{bi}[M]^2 - k_+^{bi}[M][M^*] + 2k_-^{bi}[MM] + k_-^{bi}[MM^*] \\
\frac{d[M^*]}{dt} &= k_1[M] - k_{-1}[M^*] - 2k_+^{bi}[M^*]^2 - k_+^{bi}[M][M^*] + k_-^{bi}[MM^*] + 2k_d[M^*M^*] \\
\frac{d[MM]}{dt} &= k_+^{bi}[M]^2 - k_-^{bi}[MM] + k_{-1}[MM^*] - k_1[MM] \\
\frac{d[MM^*]}{dt} &= k_+^{bi}[M][M^*] - k_-^{bi}[MM^*] + k_1[MM] - k_1[MM^*] - k_{-1}[MM^*] + k_{-1}[M^*M^*] \\
\frac{d[M^*M^*]}{dt} &= k_+^{bi}[M^*]^2 - k_d[M^*M^*] + k_1[MM^*] - k_{-1}[M^*M^*] - k_o[M^*M^*] \\
\frac{d[O]}{dt} &= k_O[M^*M^*]
\end{aligned} \qquad \text{(S1)}$$

Terms containing k_{-O} have been dropped because we assume k_{-O} =0. Solution of the full model is feasible with an ordinary differential equation solver. The initial concentration of the sum of all monomers is equal to 1 and the concentration of all other species equal to 0. The Fig. S1 shows the evolution of all the species over time for the rates given in the table below. The concentration of *O* follows bimolecular formation with the equation

$$[O] = [O]_{\max}\left(1 - \frac{1}{1 + [O]_{\max} k_f t}\right) \qquad \text{(S2)}$$

where $[O]_{max}$ = 0.5. The concentration of [*O*] for each set of parameters is fitted to Eq. (S2) and k_f is given in the Table S1.

To solve the model we must make an estimate of each rate in Eqs. (S1). The values of k_+^{bi} and k_-^{bi} can be calculated from Fick's equation of diffusion

$$K = \frac{k_+^{bi}}{k_-^{bi}} = \frac{4}{3}\pi r^3 N_A / 1000 \quad \text{(S3)}$$

$$k_+^{bi} = 4\pi r(D_M + D_{M^*})N_A / 1000 = 3.8\times10^8 \ \mathrm{M^{-1}s^{-1}} \quad \text{(S4)}$$

$$k_-^{bi} = \frac{k_+^{bi}}{K} = \frac{3(D_M + D_{M^*})}{r^2} = 9.6\times10^7 \, s^{-1} \quad \text{(S5)}$$

where r ~ 2.5 nm, the average radius of each monomer as shown in Fig. 4c, and the translational diffusion coefficients, $D_M \sim D_{M^*} \sim 1\text{x}10^{-6}$ cm^2 s^{-1} [2]. For a (arbitrary but typical) concentration of 45 μM, k_+^{bi} = 1.7 x 10^5 s^{-1}. The equilibrium of free bimolecular diffusion $K = k_+^{bi}/k_-^{bi}$=0.0019 M^{-1}, so the concentration of each of [*MM*] and [*MM**] is very low and they come apart very quickly. As can be seen in Fig. S1 the populations of these species are always very low.

We assume there are some stabilizing interactions between two *M** so that $k_d << k_-^{bi}$ but it is difficult to assess quantitatively. In Table S1 we show results of the model for k_+^{bi}/k_d= 10, 1, and 0.1, and all produce oligomer formation rates with an order of magnitude of each other. Therefore, as long as k_d is much less than the free dissociation rate, assessing this rate is not crucial.

Using a similar formalism for the intramolecular diffusion rate, we estimate the monomer reconfiguration rate from the intramolecular diffusion coefficient and the average size of the chain, $k_r = 4D/(2\langle r \rangle)^2$. Using the values in Table 1 calculated for both lengths of the peptide at pH 7.5, we calculate the reconfiguration rate at 40 C for Aβ$_{42}$ to be k_r= 4.0x10^6 s^{-1} and for Aβ$_{40}$ to be k_r= 2.2x10^7 s^{-1}. This relaxation rate is a sum of the forward and backward reconfiguration processes, $k_1 + k_{-1} = k_r$.

A parameter that is difficult to assess is the equilibrium between M and M^*, which is required for de-convolving k_1 and k_{-1}. In Table S1 we show results for k_{-1}/k_1 ranging from .1 to 10 and compare the formation rates of O for $A\beta_{42}$ and $A\beta_{40}$. The overall rates slow significantly as M^* is less populated, but the ratio of the formation rates for the two reconfiguration rates given above range from 3.7 to 5.2. Since aggregation is rare, it seems likely that M is more populated than M^*.

We also compare results for various estimates of k_O and the formation rates scale directly with this parameter. k_O is impossible to assess directly and was chosen to be $\sim 10^4$ s^{-1} to make solution of differential equations tractable. This value is almost certainly too high, but the overall formation rate of $[O]$ will scale directly with k_O, as can be seen in Table S1. If we assume k_O is the same for different sequences, comparison between Aβ lengths does not depend on an accurate estimate.

Using the rates derived above and assuming k_{-1}/k_1=0.1, k_o=1e4 s^{-1} and k_d=1.7e4 s^{-1}, we solved the Eqs. (S1) for $A\beta_{42}$ (highlighted in gray in Table S1) and $A\beta_{40}$ (highlighted in yellow in Table S1). These results are shown in Fig. S1.

Aβ length	k_1 (s^{-1})	k_{-1} (s^{-1})	k_+^{bi} (s^{-1})	k_-^{bi} (s^{-1})	k_d (s^{-1})	k_O (s^{-1})	k_f from fit ($M^{-1}s^1$)	Ratio formation rates
Comparing different estimates of k_d								
42	2e6	2e6	1.7e5	9.6e7	1.7e6	1e4	451	
42	2e6	2e6	1.7e5	9.6e7	1.7e5	1e4	755	
42	2e6	2e6	1.7e5	9.6e7	1.7e4	1e4	810	
Comparing different estimates of k_O								
42	2e6	2e6	1.7e5	9.6e7	1.7e4	1e4	810	
42	2e6	2e6	1.7e5	9.6e7	1.7e4	5e3	402	
42	2e6	2e6	1.7e5	9.6e7	1.7e4	2.5e3	199	
Comparing different estimates of k_1/k_{-1}								
42	2e6	2e6	1.7e5	9.6e7	1.7e4	1e4	810	5.2
40	1.1e7	1.1e7	1.7e5	9.6e7	1.7e4	1e4	157	
42	.8e6	3.2e6	1.7e5	9.6e7	1.7e4	1e4	85.1	4.6
40	0.44e7	1.76e7	1.7e5	9.6e7	1.7e4	1e4	18.6	
42	0.4e6	3.6e6	1.7e5	9.6e7	1.7e4	1e4	19.1	4.3
40	.22e7	1.98e7	1.7e5	9.6e7	1.7e4	1e4	4.5	
42	3.6e6	0.4et	1.7e5	9.6e7	1.7e4	1e4	9709	3.7
40	1.98e7	.22e7	1.7e5	9.6e7	1.7e4	1e4	2632	

Table S1. Various parameters used in the solution to Eqs. S8 and the fitted formation rate of [*O*].

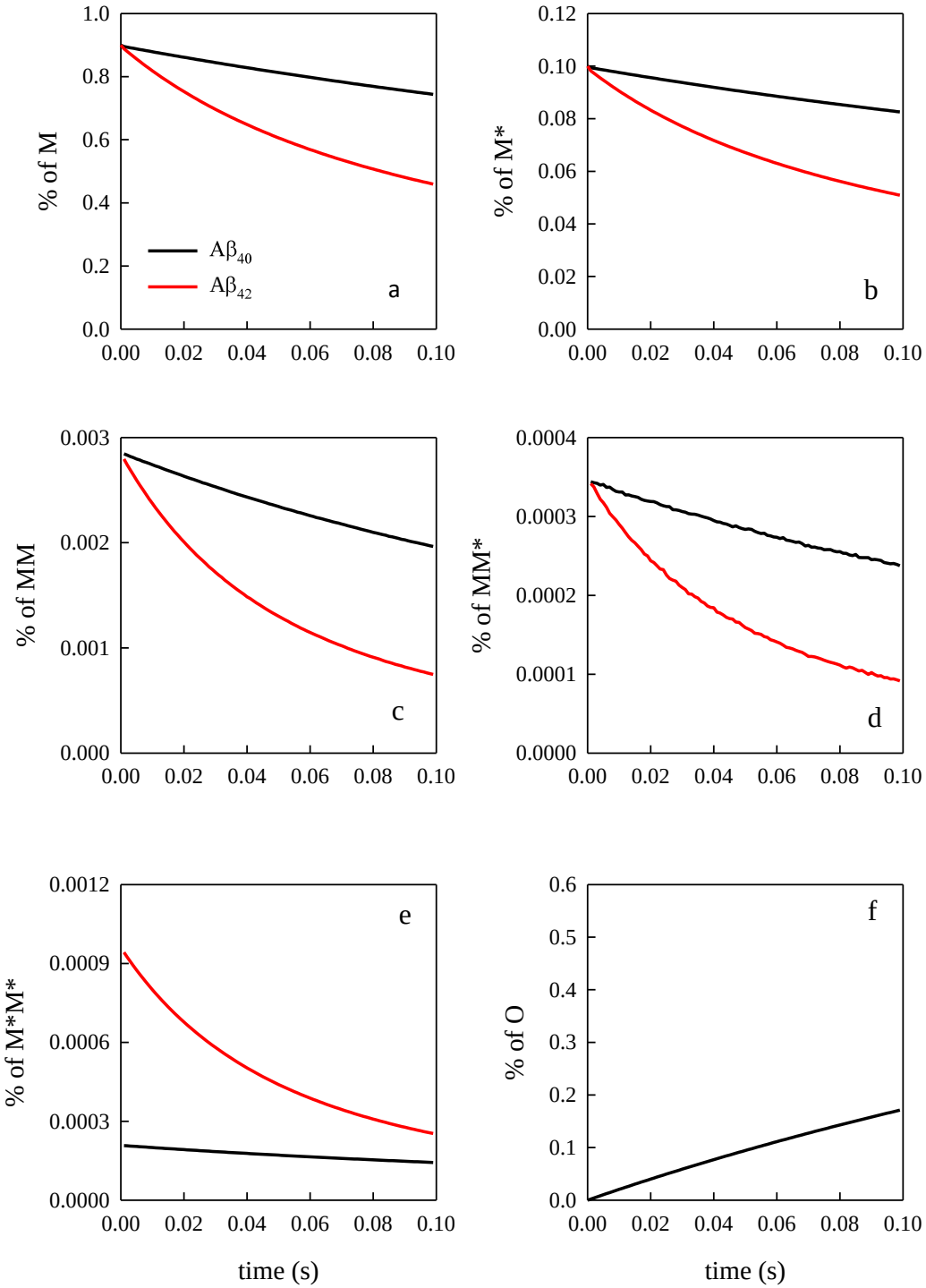

Fig. S1. Computed concentrations versus time for scheme (i) and Eq. (1) for each species (a) M, (b) M*, (c) MM, (d) MM*, (e) M*M*, (f) O. The black lines represent the aggregation of $A\beta_{40}$ and use the parameters highlighted in yellow in Table S1. The red lines represent the aggregation of $A\beta_{42}$ use the parameters highlighted in grey in Table S1.

[1] L. J. Lapidus, *Molecular BioSystems* **2013**, *9*, 29-35.
[2] L. J. Lapidus, W. A. Eaton, J. Hofrichter, *Proceedings of the National Academy of Sciences of the United States of America* **2000**, *97*, 7220-7225.